UNIVERSIDAD REGIONAL AMAZÓNICA IKIAM

Facultad de Ciencias de la Tierra y Agua

Carrera de Hidrología

Estimación de la recarga de aguas subterráneas a través de isotopos ambientales ($\delta^{2}H$ y $\delta^{18}O$) y SIG en la cuenca del río Zamora, sur de Ecuador

Alexander David Gualli Jaramillo

Tena, febrero 2022

Napo, Ecuador

Declaración de derecho de autor, autenticidad y responsabilidad

Tena, 11 de octubre de 2021

Yo, Alexander David Gualli Jaramillo con documento de identidad N° 1723469795, declaro que los resultados obtenidos en la investigación que presento en este documento final, previo a la obtención del título Ingeniero en Ciencias del Agua son absolutamente inéditos, originales, auténticos y personales.

En virtud de lo cual, el contenido, criterios, opiniones, resultados, análisis, interpretaciones, conclusiones, recomendaciones y todos los demás aspectos vertidos en la presente investigación son de mi autoría y de mi absoluta responsabilidad.

Por la favorable atención a la presente, suscribo de usted,

Atentamente,

Firma:



Alexander David Gualli Jaramillo
1723469795

INVESTIGACIÓN | Parroquia Muyuna, kilómetro 7 vía a Alto Tena
INNOVACIÓN | Tena · Napo · Ecuador
EDUCACIÓN | Telf.: (06) 370 0040 · (06) 299 9160
www.ikiam.edu.ec

Certificado de dirección de trabajo de integración curricular

Certifico que el trabajo de integración curricular titulado: "Estimación de la recarga de aguas subterráneas a través de isotopos ambientales (δ^2H y $\delta^{18}O$) y SIG en la cuenca del río Zamora, sur de Ecuador", en la modalidad de proyecto deinvestigación en formato articulo original, fue realizado por: Alexander David Gualli Jaramillo, bajo mi dirección.

El mismo ha sido revisado en su totalidad y analizado por la herramienta de verificación de similitud de contenido; por lo tanto, cumple con los requisitos teóricos, científicos, técnicos, metodológicos y legales establecidos por la Universidad Regional Amazónica Ikiam, para su entrega y defensa.

Tena, 18 de octubre de 2021

Firma:

Firmado electrónicamente por:
BRUNO PIRILO

.....

Bruno Pirilo Conicelli
C.I: 1759149774

INVESTIGACIÓN | Parroquia Muyuna, kilómetro 7 vía a Alto Tena
INNOVACIÓN | Tena · Napo · Ecuador
EDUCACIÓN | Telf.: (06) 370 0040 · (06) 299 9160
www.ikiam.edu.ec
@u_ikiam IkiamOficial u_ikiam Universidad Ikiam

Agradecimientos

A mis padres, Flavio y Rita por su amor incondicional y su apoyo para que pueda culminar mi carrera universitaria, a mis hermanos Daniela y Joel, por todo lo que hemos compartido juntos estos años y finalmente a Lio, por su peluda compañía en las largas noches de trabajo.

A mis amigos Andrea, Mishell, Ángel, Bryan, Alex, Ibeth y Diana, por estar en los buenos momentos y también en las épocas difíciles, sin ustedes, esto no hubiera sido lo mismo, los llevo en un lugar especial de mi corazón.

A los profesores de la carrera, que más que compartir su conocimiento, inspiraron en mí, esa pasión por la ciencia, en especial mi tutor Bruno, gracias por su soporte y su guía para la realización de este trabajo.

Agradezco al INAMHI, al Ministerio de Agricultura y Ganadería y al Ministerio de Ambiente y Agua que proporcionaron los datos necesarios para poder desarrollar el presente trabajo.

Dedicatoria

A mi abuelita Rosita, lamentablemente no pudiste llegar a ver como cumplía este sueño, sin embargo, fuiste la fuerza que me llevo a conseguirlo. Sin tu ejemplo de lucha, tu amor y tus consejos, nunca hubiera llegado a ser la persona que soy hoy en día, así que esto va para ti.

Índice General

1. Introducción 1

2. Descripción del sitio 3

3. Materiales and Métodos 5

3.1. Estimación de la recarga de agua subterránea utilizando un modelo de índices basado en SIG 5

3.1.1. Estimación espacial de clases de escorrentía mediante método de índice (Fase 1) 7

3.1.1.1. Mapa de permeabilidad del suelo 7

3.1.1.2. Mapa de capacidad de infiltración de la cobertura del suelo 8

3.1.1.3. Mapa de la pendiente del terreno 9

3.1.1.4. Mapa final de escorrentía superficial 9

3.1.2. Estimaciones del balance hídrico para cada una de las clases del mapa final de escorrentía superficial (Fase 2) 11

3.1.3. Mapa de recarga de agua subterránea de la cuenca del río Zamora ZRB (Fase 3) 12

3.2. Modelo conceptual de la recarga utilizando isótopos estables $\delta^{18}O$ y $\delta^{2}H$ 13

4. Resultados y discusión 14

4.1. Estimación recarga de agua subterránea utilizando un modelo de índice basado en SIG 14

4.1.1. Estimación espacial de clases de escorrentía mediante el método de índice 14

4.1.2. Estimaciones del balance hídrico para cada una de las clases del mapa final de escorrentía superficial 14

4.1.3. Mapa de recarga de agua subterránea de la cuenca del río Zamora ZRB 18

4.2. Modelo conceptual de la recarga utilizando isótopos estables $\delta^{18}O$ y $\delta^{2}H$ 21

5. Conclusiones 25

Referencias 26

Índice de tablas

Tabla 1 Clases de escorrentía y sus valores de C en el área de estudio 10

Tabla 2 Datos climatológicos utilizados para el balance hídrico en cada bloque en el periodo de 1998 a 2019 12

Tabla 3 Clasificación de las zonas de recarga de agua subterránea para la cuenca del río Zamora (ZRB) 13

Tabla 4 Composición isotópica en muestras de precipitación del proyecto ECU7007. 22

Tabla 5 Resumen estadístico de la composición de la tabla isotópica en muestras de agua de precipitación, superficial y de manantial en la cuenca del río Zamora (ZRB).....24

Índice de figuras

Fig. 1 Mapa de ubicación de la cuenca del río Zamora (ZRB) que muestra la geología y los ríos principales 4

Fig. 2 Esquema metodológico utilizado para estimar la recarga de aguas subterráneas en ZRB 6

Fig. 3 Clasificación taxonómica del suelo de la cuenca del río Zamora ZRB (A) y distribución de infiltración (B).....7

Fig. 4 Cobertura del suelo en la cuenca del río Zamora ZRB (A) y la distribución de la capacidad de infiltración(B).....8

Fig. 5 Modelo digital de elevación DEM de la cuenca del río Zamora ZRB (A) y mapa de pendientes del terreno (B) 9

Fig. 6 Mapa final de escorrentía superficial de la Cuenca del Río Zamora (ZRB) 10

Fig. 7 Bloques de precipitación y ubicación de estaciones meteorológicas para el análisis en la Cuenca del Río Zamora (ZRB).....11

Fig. 8 Sitios de muestreo de $\delta^{18}O$ y $\delta^{2}O$ en la cuenca del río Zamora (ZRB).....13

Fig. 9 Cuadro resumen de los resultados de los balances hídricos para los distintos bloques de precipitación de las distintas clases de escorrentía en la Cuenca del Río Zamora (ZRB).....17

Fig. 10 Mapa final de recarga de aguas subterráneas de la ZRB de la cuenca del río Zamora.....20

Fig. 11 LMWL y relación entre $\delta^{18}O$ y $\delta^{2}H$ en la precipitación, el agua superficial y el agua de manantial en la cuenca del río Zamora (ZRB) 23

Fig. 12 Modelo conceptual de recarga de agua subterránea para la ZRB y la media de la composición isotópica de las muestras de estudio.....24

Resumen

El manejo correcto del agua subterránea depende de la de información existente sobre sus procesos evolutivos y la caracterización de la variabilidad espacial de los mecanismos de recarga. Los modelos de índices basados en SIG se han convertido en una alternativa para mapear e interpretar modelos de recarga debido a la adaptabilidad y confianza para realizar estimaciones de recarga. Además, los isótopos estables de hidrógeno y oxígeno en el agua ($\delta^{2}H$ y $\delta^{18}O$) son útiles para determinar la procedencia y el seguimiento del agua en el ciclo hidrológico. El objetivo del estudio es contribuir al conocimiento de la recarga de aguas subterráneas mediante el desarrollo de un modelo conceptual de recarga utilizando isótopos estables y estimar la cantidad de recarga utilizando un modelo de balance hídrico espacialmente distribuido basado en SIG para la Cuenca del Río Zamora ZRB. Debido a la extensión y geografía de la cuenca, fue necesario dividirla en seis bloques de precipitación. Los resultados del análisis de una campaña de muestreo de isotopos estables para muestras de precipitación, agua superficial y agua subterránea indicaron que la precipitación es el factor más determinante la recarga de agua subterránea en la ZRB. Las altas tasas de precipitación permiten que la cuenca se cubra con zonas de recarga alta (18,22%) y moderada (30,93%). El análisis de isótopos estables en el agua ($\delta^{2}H$ y $\delta^{18}O$) indica que el agua de precipitación proviene del este, de la llanura amazónica. En los valles hay precipitación enriquecida en $\delta^{18}O$, lo que sugiere que ha pasado por un proceso de reciclaje dentro de la misma cuenca; la recarga de agua subterránea proviene de estas fuentes de precipitación.

Palabras clave: Recarga de agua subterránea, SIG, modelo de balance hídrico, isótopos estables ($\delta^{2}H$ y $\delta^{18}O$), modelo de recarga conceptual.

Abstract

The correct management of groundwater depends on the existence of information on the evolutionary processes of groundwater and the characterization of the spatial variability of recharge mechanisms. GIS-based index models have become a good alternative for mapping and interpreting recharge models due to the adaptability and confidence in making recharge estimates. Furthermore, stable isotopes of hydrogen and oxygen in water ($\delta^{2}H$ and $\delta^{18}O$) are helpful to determine the provenance and monitoring of water in the hydrological cycle. The objective of the study is to contribute to the knowledge of groundwater recharge through the development of a conceptual recharge model using stable isotopes and estimate the amount of recharge using a spatially distributed water balance model based on GIS for the Zamora River Basin ZRB. Due to the extension and geography of the basin, it was necessary to divide it into six precipitation blocks. The results of the analysis of a stable isotope sampling campaign for precipitation, surface water and groundwater samples indicated that precipitation is the most determining factor in groundwater recharge in the ZRB. The high precipitation rates make the basin covered with high (18.22%) and moderate (30.93%) recharge zones. The analysis of stable isotopes in water ($\delta^{2}H$ and $\delta^{18}O$) indicates that the precipitation water comes from the east, from the Amazon plain. Also, in the valleys, there is precipitation enriched in $\delta^{18}O$, which suggests that it has undergone a recycling process within the same basin; groundwater recharge comes from those precipitations.

Keywords: Groundwater recharge, GIS, water balance model, stable isotopes ($\delta^{2}H$ and $\delta^{18}O$), conceptual recharge mode.

1. Introduction

Understanding groundwater recharge is indispensable for successful water resources management (Healy & Scanlon, 2011). Groundwater recharge is a hydrologic process where water from the unsaturated zone infiltrates into the saturated zone below the surface of the water table (Freeze & Cherry, 1979). The recharge process occurs when water flows through the water table and seeps into the saturation zone. Many factors can affect groundwater occurrence and movement in an area, including topography, lithology, geological structure, porosity, ground cover, and climate (Fenn et al., 1975). Groundwater and aquifer research requires in situ hydrogeological experiments and geophysical research that help explain the groundwater replenishment process and help evaluate temporal and spatial differences in groundwater flows in the study area (Yeh, Lin, Lee, Hsu, et al., 2014).

Several methods estimate groundwater recharge, but none is uncertainty-free (Scanlon et al., 2002). Direct field measurements are not always representative of the entire aquifer (Hendrickx, 1992). Methods based on the Darcy equation require field measurements and numerical methods that use groundwater flow equations under full or partial saturation (Andreo et al., 2008). There are also methods based on natural tracers, either naturally dissolved compounds such as chloride balance or artificial tracers such as organic and inorganic dyes (Mazor, 2004; Wood, 1999). The disadvantage of natural tracers is that they may offer only indirect measurements of groundwater recharge, and the mechanism of infiltration may affect the interpretation of results (Allison, 1988). Another way to estimate groundwater recharge is to use water balance methods. The water input can be equal to the amount discharged plus the variation in the volume of stored water (Scanlon et al., 2002). Water balances can be estimated using semi-empirical equations using actual precipitation and temperature measurements, calculating indirect directions of existing and potential evapotranspiration and rainfall (Thornthwaite & Mather, 1955). Using the water balance approach is possible to estimate recharge rates for a large aquifer, such as at the scale of a basin (Galvão et al. 2018).

Regarding the estimates of groundwater recharge on a regional scale (size of a basin), there are studies that use flow measurements and numerical models (Nolan et al., 2007). In other cases, index methods that use GIS-based models to classify and integrate different parameters (for example, geology, drainage, soil texture, terrain slope, land cover, and lines) have helped estimate the spatial distribution of groundwater recharge (Rwanga et al. 2017). The GIS-based index is a simplified representation of the phenomenon that uses spatial data to build a model (Jasrotia et al. 2007). The GIS approach became a widespread method to estimate groundwater recharge because it

simplifies reality and extrapolates information to other areas, which can increase understanding of the system.

The GIS-based index model technique for water balance uses spatial inputs like land use, slope, and soil type. Each parameter used may have different weights according to its infiltration characteristics (Dripps & Bradbury, 2007). Depending on the purpose and hydrological characteristics of the area, the parameters used can be subjective. Many researchers use different standards to delineate theextent of potential recharge areas. Due to the inherent uncertainty of subjective selection, comparing the results of recharge estimation using other methods is recommendable (Galvão et al., 2018).

Determining the sources of groundwater recharge is essential for the effective management of groundwater resources (Yeh, Lin, Lee, Chang, et al., 2014). A widely used method to conceptualize groundwater recharge models is stable water isotopes. The stable isotopes of water ($\delta^{18}O$ and $\delta^{2}H$) are used as tracers to investigate hydrological processes such as runoff, precipitation, groundwater recharge, and the interaction of groundwater with surface water (Clark & Fritz, 1997; Gat, 1996). Comparison of the isotopic composition of $\delta^{18}O$ and $\delta^{2}H$ from precipitation and groundwater provides a tool that allows evaluating the recharge mechanism (Blasch & Bryson, 2007; Heilweil et al., 2009).

The distribution analysis of groundwater isotopes can provide information on the age and origin of the waters, identify the occurrence of mixtures between groundwater and define the environmental conditions during recharge since they act on the water throughout the hydrological cycle (Brkić et al., 2016). The stable isotope concentration distribution, known as the isotopic signature, is stable unless diluted or mixed with waters of a different isotopic composition (Liu et al., 2019). Therefore, the spatial and temporal analysis of the isotopic signatures of precipitation, surface water, and groundwater helps determine recharge zones and groundwater transit. Furthermore, this information contributes to the knowledge of the hydrological processes of the basins and is necessary for the elaboration of conceptual hydrological models (Yin et al., 2011).

In southeastern Ecuador, the Zamora River Basin (ZRB) extends from the upper part of the Andes Mountains to the Amazon plain and the Condor Mountains. The basin has a low population density; however, it suffers from high levels of anthropic pressure. The mining potential of the Condor Mountains, located in the ZRB, has allowed the establishment of a considerable number of copper and gold mines (Melo et al., 2013; van Teijlingen & Hogenboom, 2016). Mining activity has been the mainstay of economic activity in the region for decades. This activity affects relatively tiny areas but could have a significant impact on the environment. Leaks from mine tailings release heavy

metals that involve soil and surface and groundwater aquatic environments (El Khalil et al., 2008). According to some recent studies, the water quality in the basin has been affected (Mora et al., 2018, 2019; Villa-Achupallas et al., 2018).

The current growth of urban areas and the expansion of the agricultural and livestock frontier have increased deforestation processes in the basin (Torracchi, 2015). The large number of water resources required by mining, agriculture, and livestock, added to contamination with heavy metals such as Cd, Hg, and Pb from mining activities, put at risk the supply of water available for consumption by the inhabitants of the ZRB (Mora et al., 2018). An essential part of the basin's drinking water endowment is groundwater, especially spring water (Avcı & Fernández-Salvador, 2016). It becomes vital to identify recharge zones and estimate recharge values to protect water resources from anthropic activity such as pollution and land-use practices that could affect the quality and quantity of clean water for consumption.

This study aims to estimate groundwater recharge using a distributed water balance model in GIS and develop a hydrological conceptual model for the ZRB using stable isotopes ($\delta^{18}O$ and $\delta^{2}H$). This investigation is an initial exploration of the evolutionary process of groundwater in the ZRB that combines two approaches: a spatially distributed water balance model that uses GIS information (soil type, land use and slope) and the Thornthwaite & Mather water balance to estimate recharge and the use of stable isotopes ($\delta^{18}O$ and $\delta^{2}H$) for the development of a conceptual hydrological model of the basin. This approach can be useful as a starting point for further investigations using direct measurement methods.

2. Site description

The Zamora River Basin (ZRB), located between longitudes of 79°20'55" - 78°12'51"W and latitudes of 2°58'16" - 4°40'54"S in WGS 1984 (Fig. 1). The basin almost covers an area of 11.369km^2 in the southern part of the Ecuadorian Amazon. The elevation of the ZRB decreases from 4088 to 302 m.a.s.l. The ZRB has a length of 261 km. The basin is limited in the east by the Condor Mountains and the west by the Andes Mountains.

The altitudinal gradient of the ZRB has a strong influence on the climate of the basin. The different climatic levels of the basin range from the cold temperatures of the paramo regions in the higher areas, through the humid mesothermal on the eastern slope of the Andes Mountains, to the humid Tropical in the Amazon plain. The mean temperature ranges from 6°C to 25°C according to altitudinal gradient. Thus, it is June to August, the coldest, and October to December, the warmest. Despite this thermal variability, the local temperature is stable around all the year. The regional

variations between the cold and hot season its around 1.5°C to 2.5°C depending on the altitudinal gradient.

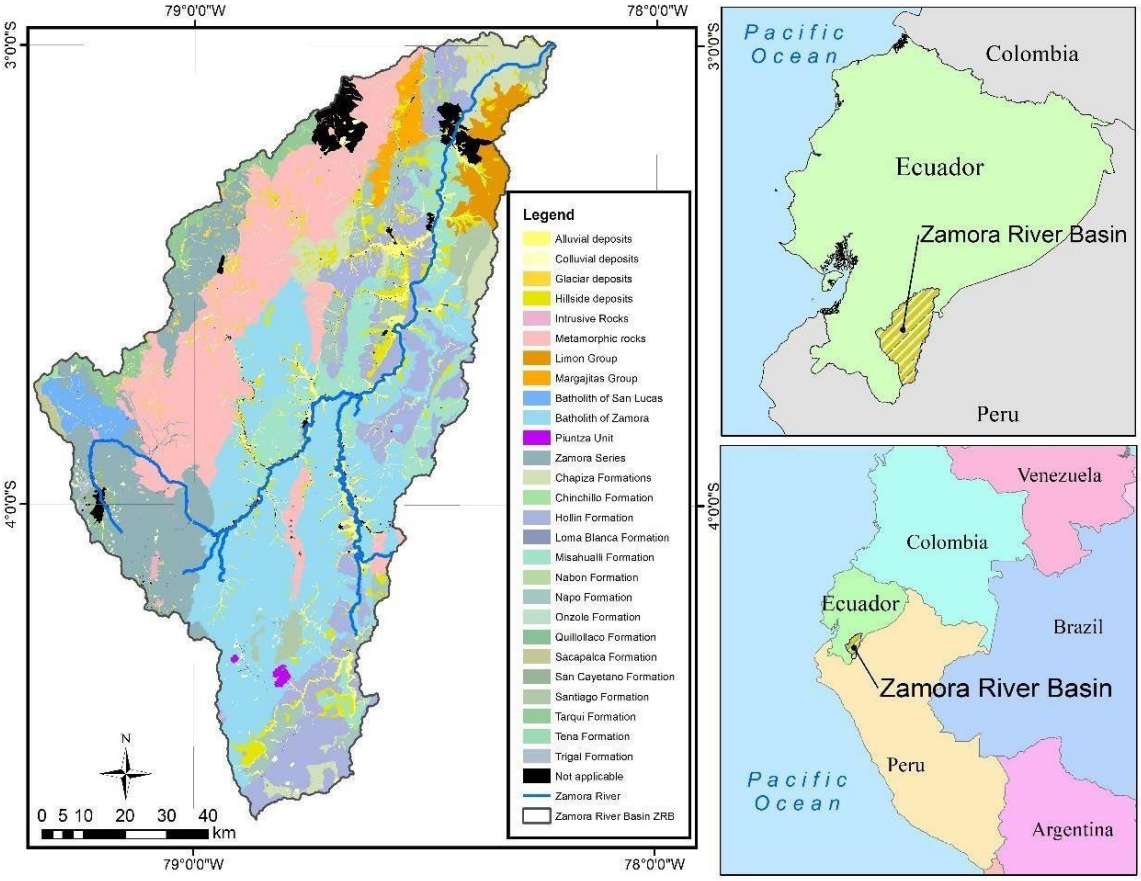


Fig. 1 Location map of Zamora River Basin showing the main geology units of ZRB and main sections of Zamora River.

Precipitation in the Andes Mountains, located on the west, has an average of 1380 mm. The months from February to April are the rainiest and the months from July to September the driest. Instead, the easternmost area, influenced by the Condor Mountains and the Cutucú Mountains, has an average annual rainfall of 1970 mm, with March to June being the highest rainfall and from November to February the lowest rainfall.

The main geological units of the basin are: in the western part, there is an extensive area covered by metamorphic rocks and the Zamora Series, in addition to the Sacapalca formation, the Tarqui formation, and the San Lucas Batholith. The Zamora Batholith and the Hollin formation cover most of the central and eastern zone, the Misahualli formation also but to a lesser extent. Finally, the northernmost sections have the Chapiza formation, the Napo formation, the Santiago formation, and the Margajitas group.

3. Materials and Methods

The methodology was divided into two parts: part 3.1 focused on developing the estimation of groundwater recharge using a GIS-based index model and part 3.2 focused on the realization of a conceptual model of groundwater recharge using stable isotopes.

3.1. Groundwater recharge estimation using GIS-based index model

The GIS-based index method for distributed recharge integrates the water balance adapted from (Galvão et al., 2018). The first phase consisted in building a surface runoff map, overlay maps of land cover, soil, and terrain slope classified in their permeability capacities. The second phase used the water balance method adapted from Thornthwaite & Mather, (1955) to estimate groundwater recharge values for different water percolation scenarios. Finally, in the third phase, the water percolation flow values were used to develop the map of the groundwater recharge zone. A schematic representation and a detailed explanation of the adaptation of the method Galvão et al., (2018) are presented in Fig. 2.

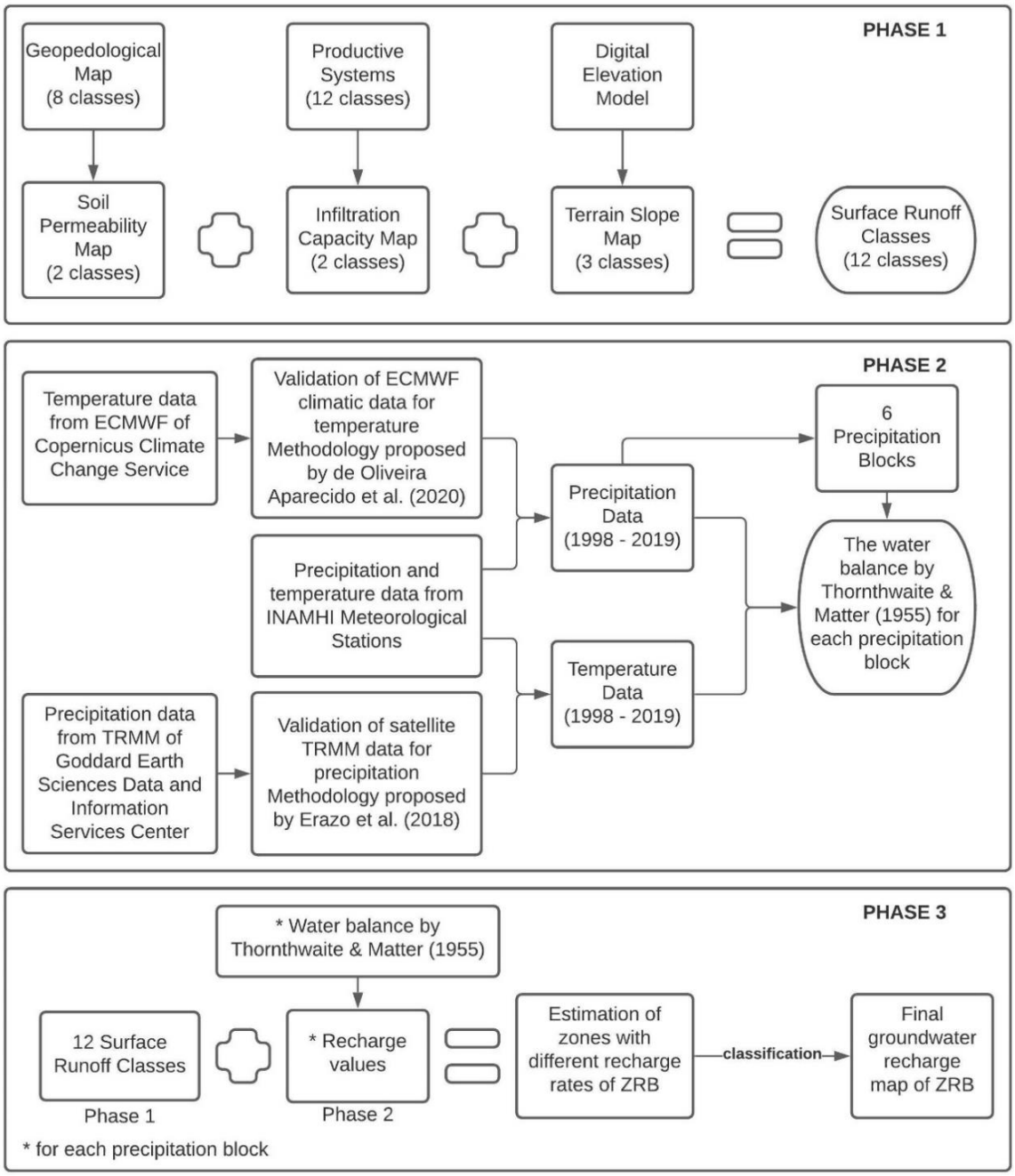


Fig. 2 Methodological scheme used to estimate the groundwater recharge in ZRB with the GIS-based index model. Phase 1: establish the surface runoff classes of the basin soil. Phase 2: establish the precipitation blocks (basin areas with similar precipitation values), treatment and validation of meteorological and reanalysis data, and the respective Thornthwaite & Mather water balance for each precipitation block, to obtain groundwater recharge values. Phase 3: spatial distribution of the groundwater recharge values from the water balance (phase 2) to the surface runoff classes (phase 1) and its classification according to ratios.

3.1.1. Estimating runoff classes spatially by index method (Phase 1)

3.1.1.1. Soil permeability map

The layer of soil taxonomic classification for the Zamora Basin comes from the Geopedological map of continental Ecuador of MAGAP. This layer characterizes the area in ten different taxonomic types of soils: alfisols, andisols, entisols, histosols, inceptisols, mollisols, ultisols, vertisols (Fig. 3a). Also, this GIS information found two classes called not applicable and miscellaneous lands, defined as populated areas, bodies of water, wastelands, anthropic infrastructure, and lands that are not considered land units or taxonomic units. The characteristic percentages of clay, sand, or silt of each of the taxonomic classes of the soil determined the reclassification. According to our new classification, impermeable soils have low silt content and few clay particles, while moderately permeable soils have high clay particles and high silt content. With these considerations, the reclassification of the new map of soil permeability was elaborated using three soil permeability classes: (1) silty (low permeability or high runoff) and (2) clayey (almost no permeability and high runoff)(Fig. 3b).

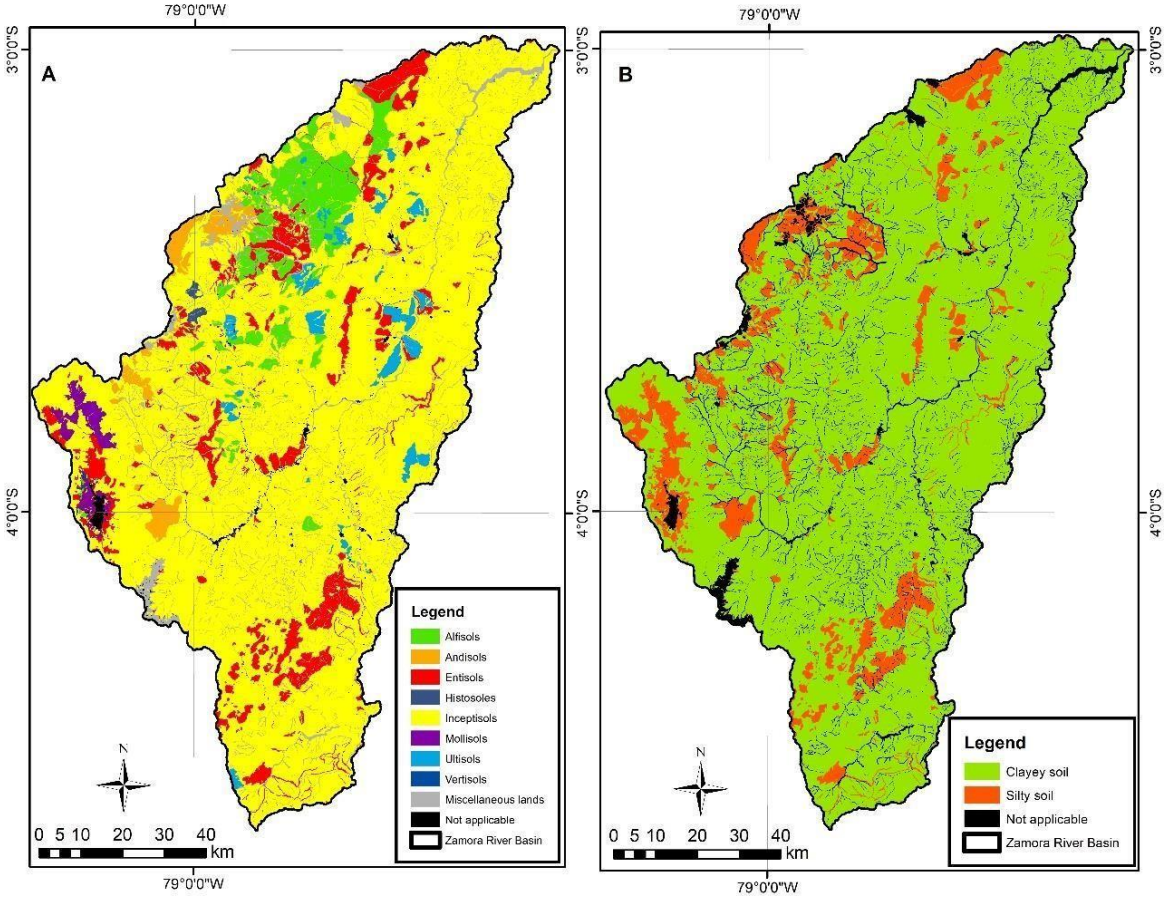


Fig. 3 Soil taxonomic classification of Zamora River Basin ZRB (A) and the distribution of soil permeability classes (B)

3.1.1.2. Land cover infiltration capacity map

The land-use layer was elaborated by the Ecuador Productive Systems 1:25000 of MAGAP. This classification characterized the area in twelve different land-use types: agricultural mosaic, anthropic infrastructure, crops, a forest plantation, herbaceous vegetation, native forest, paramo, pastureland, populated area, shrubby vegetation, wasteland, and water body (excluded from the analysis) (Fig. 4a). These land-use types were reclassified in two classes based on their infiltration rates to develop an infiltration capacity map. The two infiltration capacity classes were (1) forest and paramo (high permeability or low runoff) and (2) anthropic structures, crops, and pastures (low permeability or high runoff). The forest and paramo soil permeability class grouped native forest, forest plantations, shrubby vegetation, and paramo. The anthropic structures, crops, and pastures soil permeability class were grouped into the remaining seven categories (Fig. 4b).

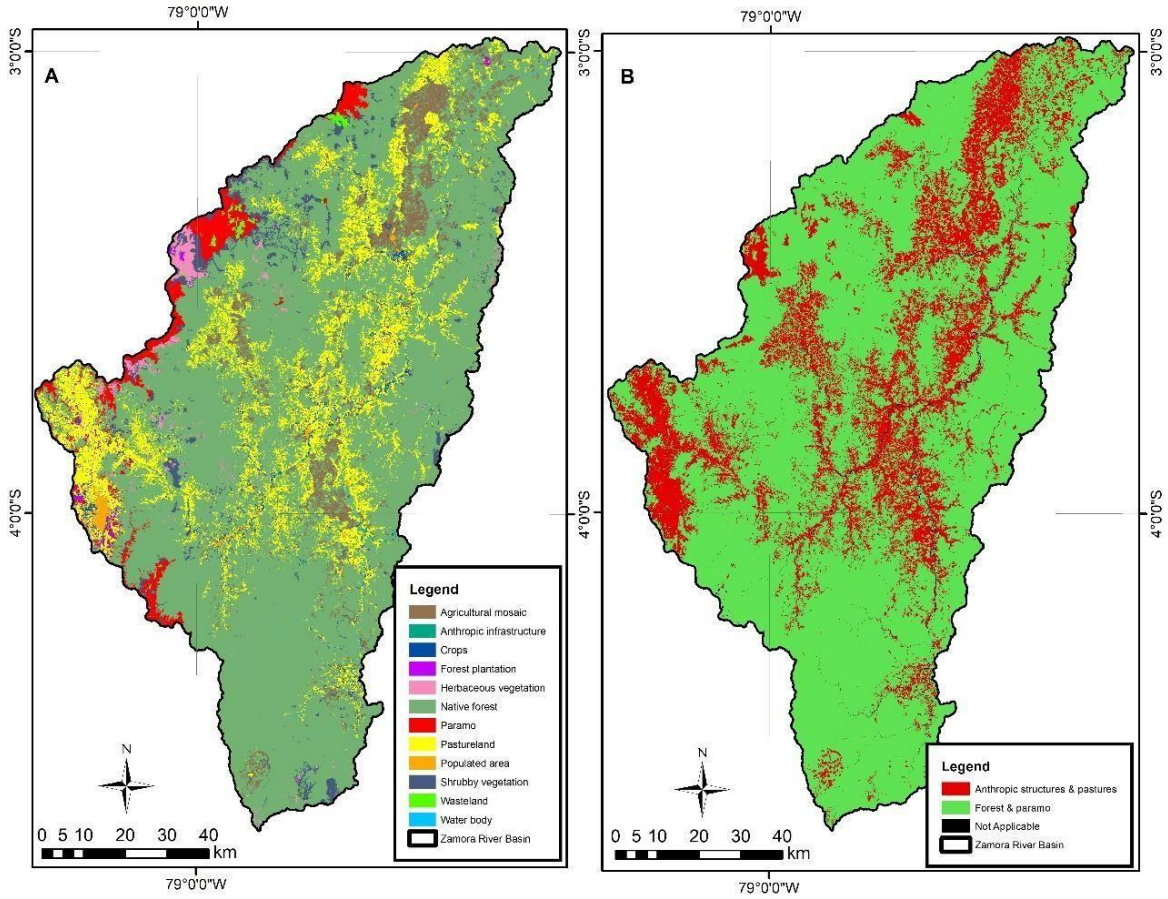


Fig. 4 Land cover of Zamora River Basin ZRB (A) and distribution of infiltration capacity classes (B)

3.1.1.3. Terrain slope map

The slope of the land in percentage comes from the processing of a DEM acquired from SIG Tierras elaborated by the MAGAP. The DEM pixel resolution was 3x3 m (Fig. 5a). Three slope intervals were defined, according to the ASCE-American Society of Civil Engineers, (1969): < 2%— low slopes; 2–7%—moderate slopes; and> 7%—high slopes (Fig. 5b).

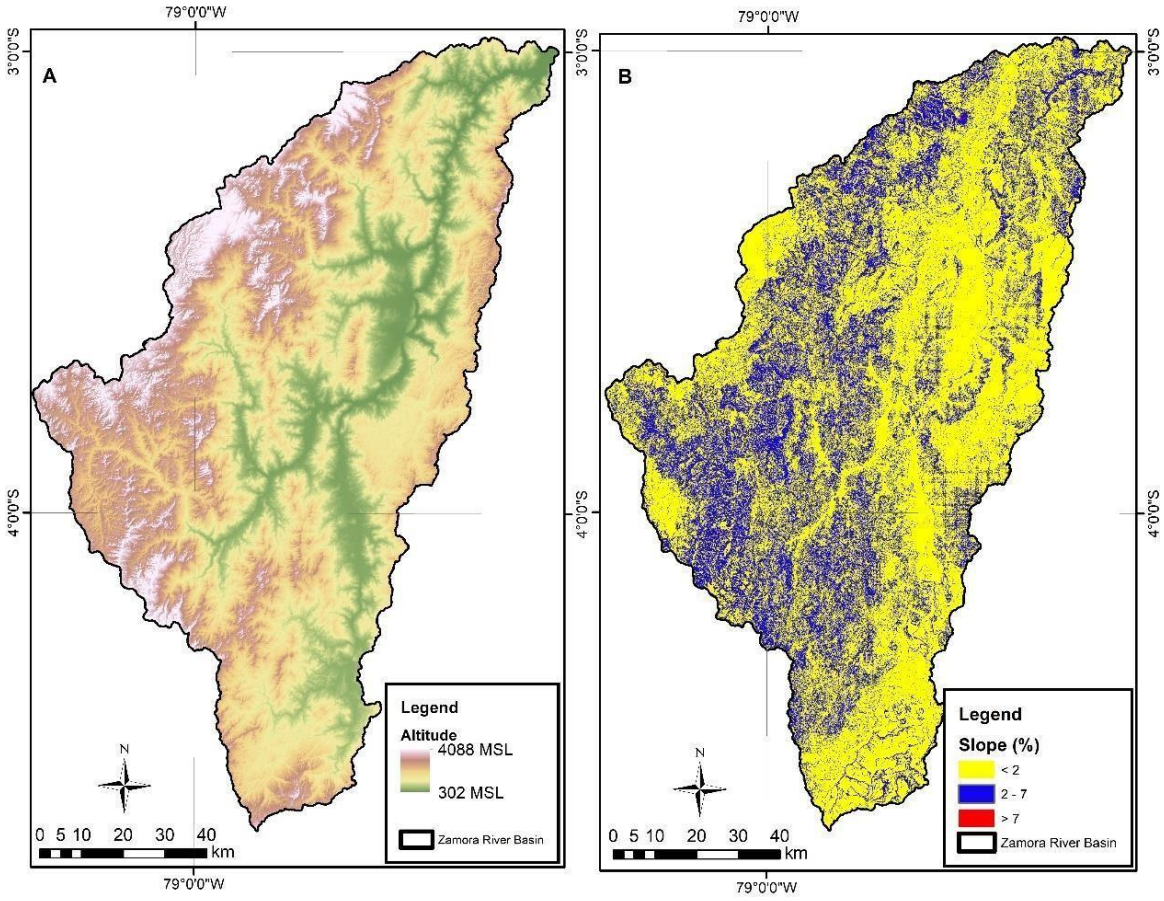


Fig. 5 Digital Elevation Model of Zamora River Basin ZRB (A) and the terrain slope map indicating predominance for slopes < 7 (B)

3.1.1.4. Final surface runoff map

The three shapefiles: soil permeability (Fig. 3), land cover infiltration capacity (Fig. 4), and terrain slope (Fig. 5), were georeferenced in a GIS database in QGIS 3.10.2. The shapefiles were then converted to a 3x3m pixel raster format (matching the DEM resolution) and then integrated into the QGIS raster calculator using the formula to calculate the runoff coefficient (Table 1). Finally, the surface runoff was estimated using twelve surface runoff classes (Table 1). The coordinate system used was UTM projection, Zone 17S, datum WGS 1984, with units in meters (Fig. 6).

Table 1 Runoff classes and their values of C in the study area. The lower the runoff coefficient, the higher the permeability capacity, and the higher the runoff coefficient, the lower the permeability capacity. The values of C, C1 ', C2' and C_3' according to the methodology of Galvão (2018).

Runoff Classes	Soil Permeability	Land Cover Infiltration Capacity	Terrain Slope (%)		Runoff Coefficient
	C'_1	C'_2	C'_3	$C = 1 - (C'_1+C_2+C'_3)$	C
Class 1	Silty	Forest and Paramo	< 2	1 - (0.2+0.2+0.3)	0.3
Class 2			2-7	1 - (0.2+0.2+0.2)	0.4
Class 3			>7	1 - (0.2+0.2+0.1)	0.5
Class 4		Anthropic structures, crops and pastures	< 2	1 - (0.2+0.1+0.3)	0.4
Class 5			2-7	1 - (0.2+0.1+0.2)	0.5
Class 6			>7	1 - (0.2+0.1+0.1)	0.6
Class 7	Clayey	Forest and Paramo	< 2	1 - (0.1+0.2+0.3)	0.4
Class 8			2-7	1 - (0.1+0.2+0.2)	0.5
Class 9			>7	1 - (0.1+0.2+0.1)	0.6
Class 10		Anthropic structures, crops and pastures	< 2	1 - (0.1+0.1+0.3)	0.5
Class 11			2-7	1 - (0.1+0.1+0.2)	0.6
Class 12			>7	1 - (0.1+0.1+0.1)	0.7

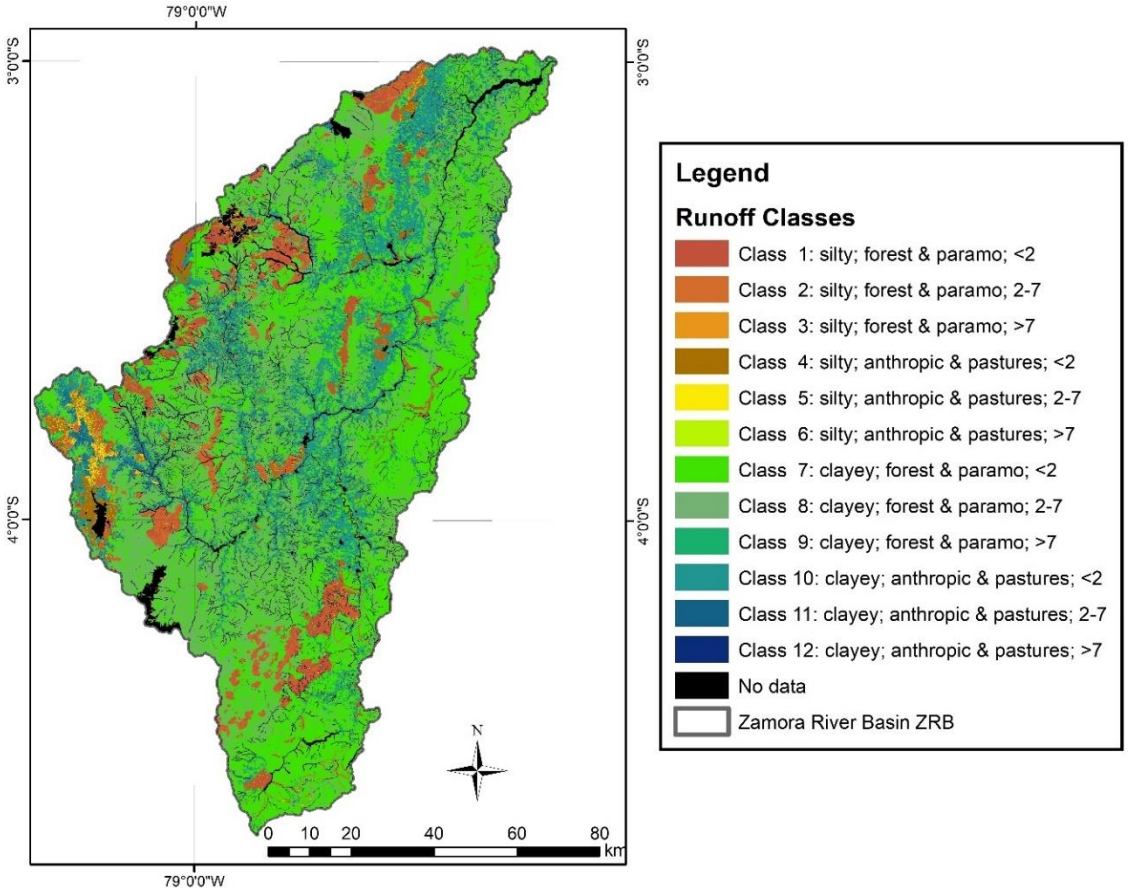


Fig. 6 Final surface runoff map of the Zamora River Basin (ZRB). The runoff classes are result of the integration of maps of soil permeability, infiltration capacity, and terrain slope.

3.1.2. Water balance estimations for each class of the surface runoff map (Phase 2)

The water balance was estimated using temperature and precipitation data retrieved from the INAMHI meteorological stations. Despite the vast area of the basin (< 11 000 km^2), ZRB has only historically recorded precipitation and temperature data from 5 stations (Fig. 7). We used reanalysis data to compensate for the lack of historical data and complement the spatial analysis of precipitation and temperature. The climate reanalysis data were calibrated and used as a proxy to reproduce local climate variability. Data from ECMWF Copernicus Climate Change Service, (2017) were used to estimate surface air temperature (2 m temperature) and from TRMM Tropical Rainfall Measuring Mission, (2011) for precipitation data. We defined five points to spatially locate the reanalysis results; the location of these points depended on spatial parameters of distance and representativeness (Fig. 5). The reanalysis data were validated using the methodology proposed by Erazo et al. (2018) for precipitation and the methods proposed by de Oliveira Aparecido et al. (2020) for temperature.

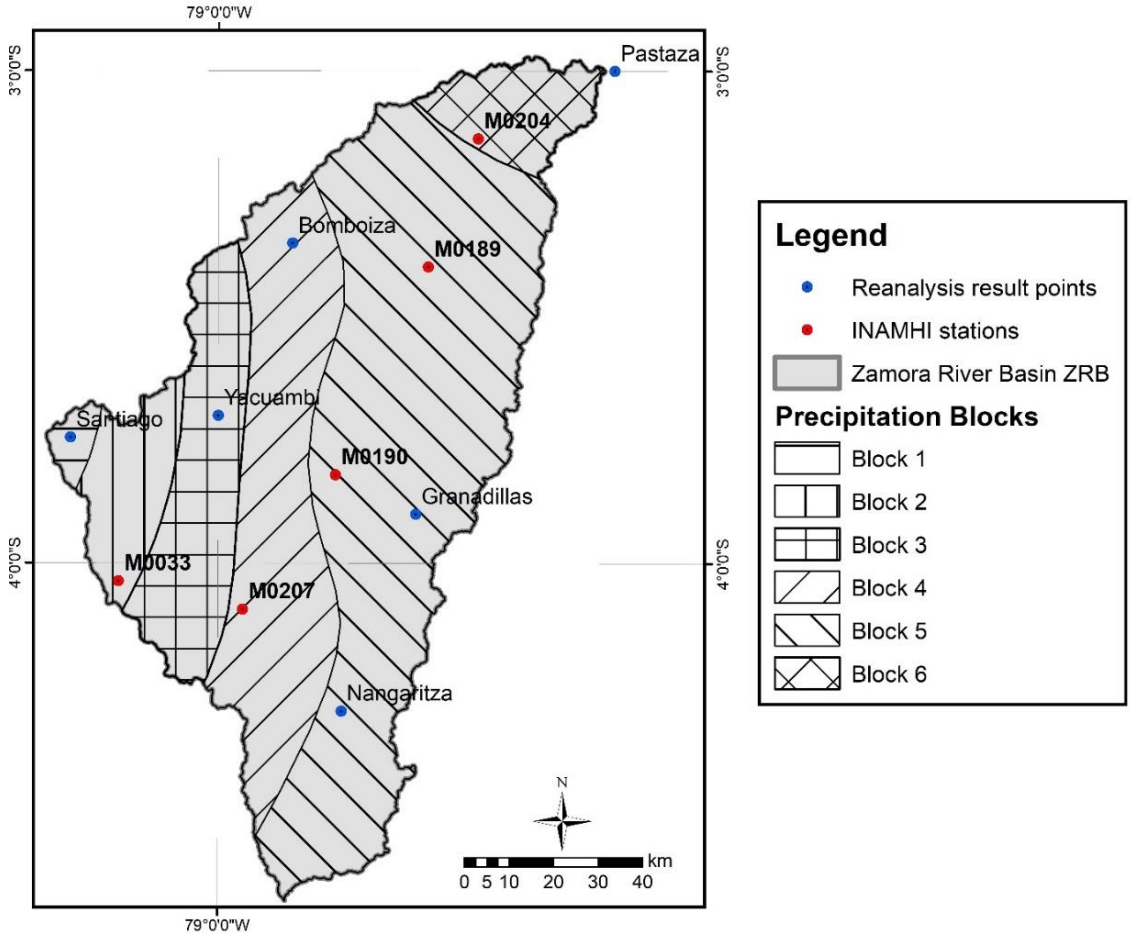


Fig. 7 Precipitation blocks and ubication of meteorological stations for the analysis in Zamora River Basin (ZRB)

Due to the extension of the basin, the water balance was estimated in six precipitation blocks. With the interpolation of precipitation data from real stations and reanalysis results points, we define six precipitation blocks. We carried out the water balance for the twelve classes of surface runoff from each of these six blocks using the methodology proposed by Pereira (2005) in the period from 1998 to 2019.The data averages from the INAMHI climatological stations and reanalysis result points within each block characterized each block's temperature and precipitation values (Table 2).

Table 2 Climatological data used for water balance in each block in the period from 1998 to 2019. The monthly values for each precipitation block are the average of the data from meteorological stations and the reanalysis result points.

Mean precipitation 1998 – 2019 (mm)												
	Jan	**Feb**	**Mar**	**Apr**	**May**	**Jun**	**Jul**	**Aug**	**Sep**	**Oct**	**Nov**	**Dec**
Block 1	83	96	111	76	68	60	54	38	45	61	58	67
Block 2	98	130	145	98	68	58	52	40	38	80	73	95
Block 3	118	132	175	143	115	100	66	54	71	74	83	94
Block 4	143	161	197	179	131	103	88	79	87	101	114	131
Block 5	142	145	190	193	186	185	144	106	121	132	127	135
Block 6	168	146	220	217	207	237	176	142	150	145	149	136
Mean temperature 1998 – 2019 (°C)												
	Jan	**Feb**	**Mar**	**Apr**	**May**	**Jun**	**Jul**	**Aug**	**Sep**	**Oct**	**Nov**	**Dec**
Block 1	14.8	14.8	14.8	15.0	14.9	14.2	13.7	14.3	15.1	14.9	14.6	14.7
Block 2	16.2	16.3	16.5	16.6	16.4	15.7	15.2	15.6	16.2	16.6	16.7	16.5
Block 3	19.7	19.8	20.0	20.1	19.9	19.2	18.7	19.1	19.7	20.1	20.2	20.0
Block 4	22.8	22.8	22.8	22.6	22.2	21.2	20.7	21.1	22.0	22.8	23.2	23.1
Block 5	23.6	23.4	23.5	23.4	23.0	22.1	21.6	21.9	22.6	23.5	24.0	23.8
Block 6	18.8	18.8	18.9	18.8	18.5	17.7	17.3	17.9	18.5	18.8	18.9	18.7

3.1.3. Groundwater Recharge Map of Zamora River Basin ZRB (Phase 3)

We used phases one and two products to estimate the areas of different recharge rates in the ZRB (Fig. 2). The final surface runoff map (Fig. 6) showed the twelve soil classes according to their potential recharge capacity. This map added the information on the annual recharge ratio obtained through the water balances for the flow of one of the six precipitation blocks, and spatial distribution of the groundwater recharge for the entire basin is obtained. We categorized the spatial distribution of recharge in four regions according to the annual recharge capacity (Table 3) to get the final ZRB groundwater recharge map (Fig. 10).

Table 3 Classification of groundwater recharge zones for the Zamora River Basin (ZRB)

Recharge Zone		Recharge Ratio
Zone 1	High recharge values	>100 mm/yr
Zone 2	Moderate recharge values	50-100 mm/yr
Zone 4	Low recharge values	25-50 mm/yr
Zone 5	Incipient recharge values	<25 mm/yr

3.2. Recharge Conceptual Model using stable isotopes $\delta^{18}O$ and $\delta^{2}H$

The data from stable isotopes $\delta^{18}O$ and $\delta^{2}H$ came from the ECU7007 project "Strengthening the Management and Water Quality Control of the Zamora River Basin through the Application of Isotope Techniques." The data include two water stable isotopes sampling campaigns. The campaigns were carried out in January (for wet season) and September (for dry season) 2018. The sampling sites were: five precipitation points, seventeen superficial points, and ten spring water points (Fig. 8). For this study, we only had access to isotopic information from the first campaign.

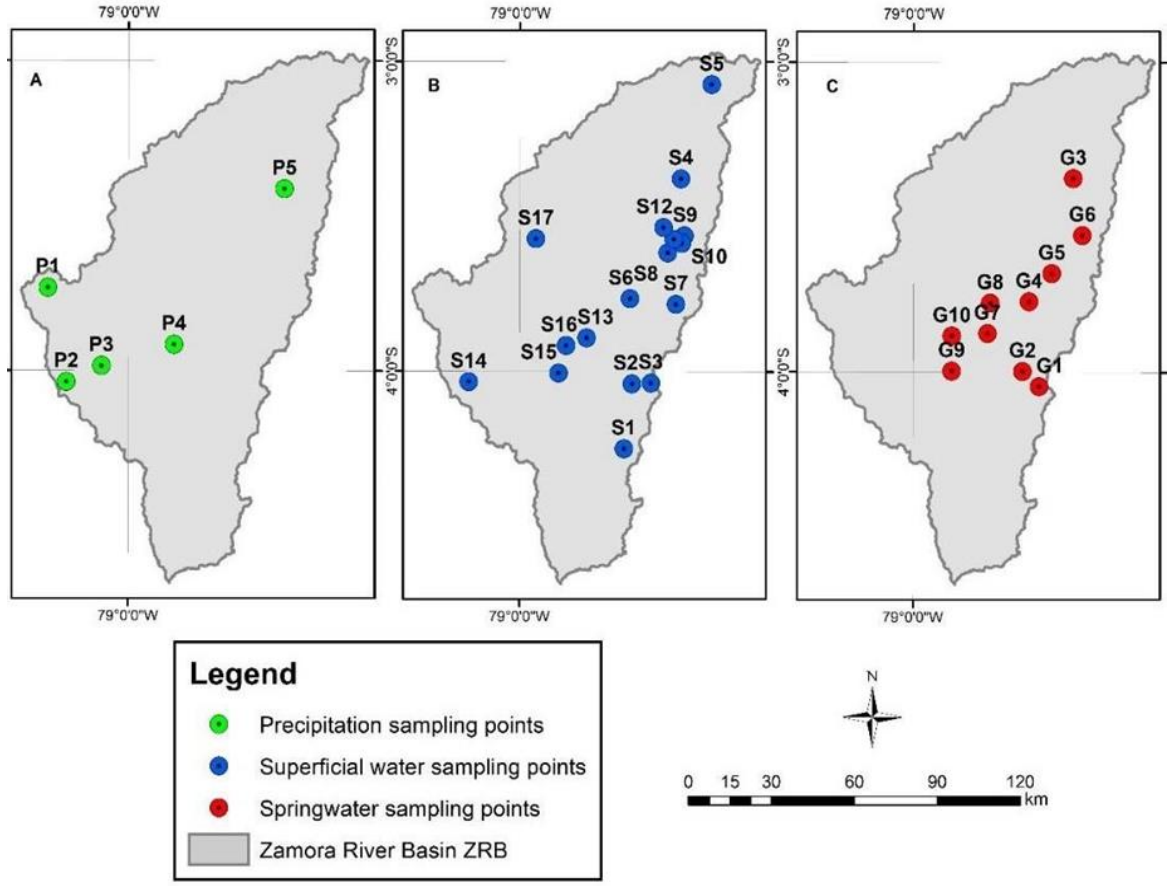


Fig. 8 Sampling sites of $\delta^{18}O$ and $\delta^{2}H$ in Zamora River Basin (ZRB). Precipitation samples (A), surface water samples (B), and spring water samples (C).

4. Results and discussion

4.1. Groundwater recharge estimation using GIS-based index model

4.1.1. Estimating runoff classes spatially by the index method

Clayey soils constitute the majority of the basin soil, mainly inceptisols that cover ~75% of the ZRB area. There are also siltysoils distributed in patches around the entire basin, and there are no sandy soils within the basin (Fig. 3). The predominant presence of clay soils (~ 82%), implies a waterproofing effect that generates high runoff and hinders high groundwater recharge rates in the ZRB (Koerner & Daniel, 1997).

Most of the ZRB area is covered by native forest (~70%), followed by grasslands (14%) and agricultural mosaics (4.8%) concentrated around populated sites and river stretches. The infiltration capacity map (Fig. 4b) reveals that reclassification locates most of the basin as a class of forest and paramo associated with high potential permeability. The westernmost part of the ZRB concentrates places of high groundwater recharge such as paramos. The other classifications such as forest plantations and shrub vegetation each occupy an area less than 0.2% of the basin. The class anthropic structures, crops, and pastures are distributed throughout the watershed, especially the plains covered by pastureland near rivers and populated areas.

The watershed has a maximum altitude of 4088 m.a.s.l. to a minimum of 302 m.a.s.l. (Fig. 3a). That is an altitude variation of almost 3,800 meters and an average slope of 1.6%. Flat areas, <2%, cover approximately 69.23% of the ZRB, followed by areas with moderate slopes, 2-7%, representing 30.7%, and a practically imperceptible number of sites with high slopes > 7%, almost 0.07%. Despite the enormous altitudinal variation in the basin, there are almost no areas with a high slope. To explain the low slopes in a large altitudinal gradient, the hypsometric curve of the basin was revised, which indicated that it has reached equilibrium and is in the maturity phase, which did not explain the observation of low slopes in the ZRB. Slopes may decrease as resolution increases. So, it was attributed to low slopes that may be biased given the resolution of the digital elevation model DEM (Chang & Tsai, 1991).

4.1.2. Water balance estimations for each class of the surface runoff map

The description of groundwater recharge in ZRB is in Fig. 9, and the area distributions are shown in Fig. 10. The integration of the twelve surface runoff classes with the six precipitation blocks generated seventy-two recharge areas. The results (Fig. 9) indicated that for precipitation block one, the recharge values for runoff classes one and two are between incipient (9 mm/yr) and low (30 mm/yr). The rest of the runoff classes had incipient recharge values (< 9 mm/yr). In precipitation

block one, clay soils (Fig. 3b) and moderate annual precipitation of 818.7 mm/yr (Table 2) did not provide the necessary conditions for significant groundwater recharge. Precipitation block two (Fig.9) has an annual rainfall of 976 mm/yr and registered recharge values between 9 and 80 mm/yr for all classes except for runoff classes six, eleven, and twelve. Runoff class one has a moderate discharge rate, while runoff classes two, four, and seven had low recharge rates. The rest of the runoff classes had incipient recharge values.

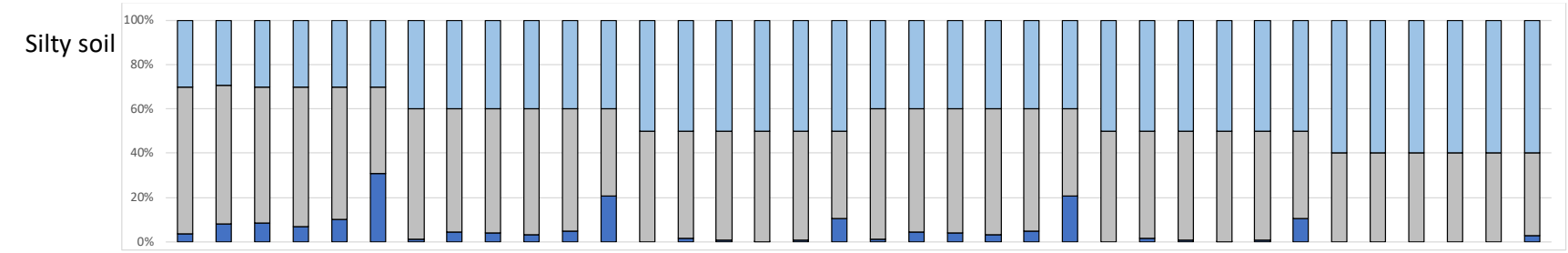
Precipitation blocks three and four (Fig.9) had an annual rainfall of 1226 and 1514 mm/yr, respectively (Table 2), and recorded maximum recharge values of 105 and 106 mm/yr, respectively; this recharge ratio was for runoff class one. Both precipitation blocks registered low recharge values (47 mm/yr) for runoff classes two, four, and seven and incipient (2 and 11 mm/yr) for runoff classes three, five, eight, and ten. No recharge was registered for runoff classes six, nine, eleven, and twelve. The groundwater recharge in precipitation blocks three and four has similar values in all runoff classes, even considering a precipitation difference of 288 mm/yr. The differentiating factor between these precipitation blocks was the temperature, 19.7 °C for precipitation block three and 22.3 °C for precipitation block four. In the Thornthwaite & Mather (1955) method, evapotranspiration is directly linked to temperature. The temperature difference of 2.6 °C between blocks three and four was reflected in the evapotranspiration values. The higher temperature of block four increased the evapotranspiration values and canceled the effect of the additional precipitation that this block has.

Finally, precipitation blocks five and six had (Fig.9) an annual rainfall of 1805 and 2092 mm/yr (Table 2) and maximum recharge values of 184 and 642 mm/yr, respectively. Runoff class one has the highest recharge values. Precipitation block five has high recharge values (85 mm/yr) for runoff classes two, four, and seven; it has incipient recharge (11 mm/yr) for runoff classes three, five, eight, and ten. Runoff classes six, nine, and eleven did not have a recharge. Precipitation blocks six has high recharge values (642, 433, and 223 mm/yr) for runoff classes one, two, three, four, five, seven, eight, and ten, high recharge values (55 mm/yr) for runoff classes six, nine and eleven and class twelve has no recharge.

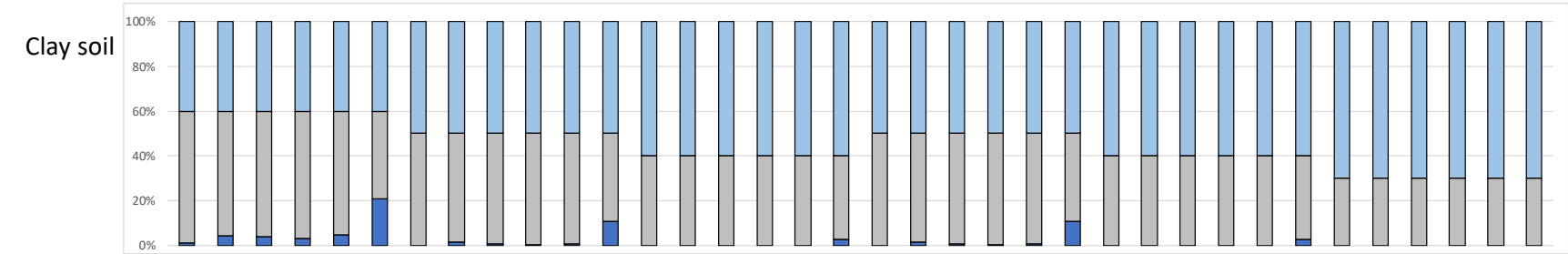
The recharge values of precipitation block six were very different from those of the rest of the precipitation blocks. The high recharge values for precipitation block six were related to the fact that it has an average annual rainfall of 2,092 mm/yr (Table 2), the highest in the ZRB. In addition, the temperature of this block has an annual average of 18.5 °C; this is on average 4 °C colder than that of blocks four and five. Lowerevapotranspiration values implied higher percolation values (Koerner & Daniel, 1997). The high precipitation and low evapotranspiration (due to the low

temperature) caused the unusual and high recharge rate for this precipitation block.

In Galvão's (2018) methodology for soil permeability, the soil composition (sandy, silty and clayey) was the factor with the most significant weight when determining its permeability. The soils of the ZRB were only composed of loamy and clayey soils with low permeability; however, it has favorable characteristics for recharge, such as slopes <7% (Fig. 5) and native forest cover (Fig. 4). These characteristics increased the probability of groundwater recharge for the ZRB. It is also important to highlight that despite the importance of soil characteristics in recharge processes (Fig. 9), annual precipitation was the most significant individual driver of groundwater recharge, as indicated by (Conicelli et al., 2021).



Precipitation (mm/yr)	819	976	1227	1514	1806	2092	819	976	1227	1514	1806	2092	819	976	1227	1514	1806	2092	819	976	1227	1514	1806	2092	819	976	1227	1514	1806	2092	819	976	1227	1514	1806	2092
Recharge (mm/yr)	30	80	105	106	184	642	9	42	47	47	85	433	0	14	9	2	11	223	9	42	47	47	85	433	0	14	9	2	11	223	0	0	0	0	0	55
Evapotranspiration (mm/yr)	543	619	754	954	1080	823	482	544	689	861	998	823	409	474	604	755	892	823	482	544	689	861	998	823	409	474	604	755	892	823	327	390	491	606	722	782
Runoff (mm/yr)	246	293	368	454	542	628	327	390	491	606	722	837	409	488	613	757	903	1046	327	390	491	606	722	837	409	488	613	757	903	1046	491	586	736	909	1083	1255
Precipitation Block	**B1**	**B2**	**B3**	**B4**	**B5**	**B6**	**B1**	**B2**	**B3**	**B4**	**B5**	**B6**	**B1**	**B2**	**B3**	**B4**	**B5**	**B6**	**B1**	**B2**	**B3**	**B4**	**B5**	**B6**	**B1**	**B2**	**B3**	**B4**	**B5**	**B6**	**B1**	**B2**	**B3**	**B4**	**B5**	**B6**
	Runoff Class 1 (slope <2%)						**Runoff Class 2** (slope 2%-7%)						**Runoff Class 3** (slope >7%)						**Runoff Class 4** (slope <2%)						**Runoff Class 5** (slope 2%-7%)						**Runoff Class 6** (slope >7%)					



Precipitation (mm/yr)	819	976	1227	1514	1806	2092	819	976	1227	1514	1806	2092	819	976	1227	1514	1806	2092	819	976	1227	1514	1806	2092	819	976	1227	1514	1806	2092	819	976	1227	1514	1806	2092
Recharge (mm/yr)	9	42	47	47	85	433	0	14	9	2	11	223	0	0	0	0	0	55	0	14	9	2	11	223	0	0	0	0	0	55	0	0	0	0	0	0
Evapotranspiration (mm/yr)	482	544	689	861	998	823	409	474	604	755	892	823	327	390	491	606	722	782	409	474	604	755	892	823	327	390	491	606	722	782	246	293	368	454	542	628
Runoff (mm/yr)	327	390	491	606	722	837	409	488	613	757	903	1046	491	586	736	909	1083	1255	409	488	613	757	903	1046	491	586	736	909	1083	1255	573	683	859	1060	1264	1465
Precipitation Block	**B1**	**B2**	**B3**	**B4**	**B5**	**B6**	**B1**	**B2**	**B3**	**B4**	**B5**	**B6**	**B1**	**B2**	**B3**	**B4**	**B5**	**B6**	**B1**	**B2**	**B3**	**B4**	**B5**	**B6**	**B1**	**B2**	**B3**	**B4**	**B5**	**B6**	**B1**	**B2**	**B3**	**B4**	**B5**	**B6**
	Runoff Class 7 (slope <2%)						**Runoff Class 8** (slope 2%-7%)						**Runoff Class 9** (slope >7%)						**Runoff Class 10** (slope <2%)						**Runoff Class 11** (slope 2%-7%)						**Runoff Class 12** (slope >7%)					

Forest and Paramo Anthropic structures, crops and pastures

Fig. 9 Summary table of the results of the water balances for the different precipitation blocks of the different runoff classes in the Zamora River Basin (ZRB). B1, B2, B3, B4, B5, and B6 indicate each precipitation block as established in section 3.1.2. At the top the runoff classes with silty soils and at the bottom the runoff classes with clay soils. In green the runoff classes with a cover of forest and paramo and yellow the runoff classes with a cover of anthropic structures, crops, and pastures. Groundwater recharge values for the different runoff classes in each precipitation block are marked with blue.

4.1.3. Groundwater Recharge Map of Zamora River Basin ZRB

Zone 1 (blue, Fig. 10) represents 18.22% of the basin registered high recharge rates, with values greater than 100 mm/yr. Includes runoff class one of the precipitation blocks three, four, and five and runoff classes one, two, three, four, five, seven, eight, and ten of precipitation block six. This area can be found mainly at the mouth of the basin, in the northern part of the ZRB, which is precipitation block six, distributed in patches in the central and northern part of precipitation blocks four and five and small areas in the center precipitation block three. It occurs when C = 0.3 in precipitation blocks three, four, and five and when C = 0.4 - 0.5 (Table 1) in precipitation block six.

Zone 2 (green, Fig. 10) represents 30.93% of the basin, this zone registered moderate recharge rates with values between 50 and 100 mm/yr. Includes runoff class one of precipitation block two, classes two, four, and seven of precipitation block five, and runoff classes six, nine, and eleven of precipitation block six. It occurs when C = 0.3 in precipitation block two, when C = 0.4 in precipitation block five, and when C = 0.6 in precipitation block six (Table 1). This zone can be seen as small scattered patches in the northwestern part of precipitation block six, covering most of the whole of precipitation block five and scattered zones in the north and south part of precipitation block two.

Zone 3 (yellow, Fig. 10) represents 18.82% of the basin registered low recharge rates with values from 25 to 50 mm/yr. Includes runoff class one of precipitation block one and runoff classes two, four, and seven of precipitation blocks two, three, and four. It occurs when C = 0.3 in precipitation block one and when C = 0.4 in precipitation blocks two, three, and four (Table 1). This zone can be identified as several small zones scattered in precipitation blocks one, two, three, and four of the ZRB.

Zone 4 (orange, Fig. 10) represents 32.04% of the basin registered incipient recharge rates, with values lower than 25 mm/yr. Includes the remaining runoff classes of all blocks. It occurs when C = 0.7 in all precipitation blocks, when C = 0.5 - 0.6 in precipitation blocks one to four and when C = 0.4 in precipitation block one (Table 1). This area is distributed as scattered patches around the entire basin, except in precipitation block six.

It is also essential to consider that although some areas have low recharge rates and high surface runoff, they are close to areas of high and moderate recharge rates, therefore the water drained from areas of high recharge located at a higher elevation it can reach areas with low percolation (Galvão et al., 2018). Although the ZRB is covered with clayey and silty soil, the low slopes, the coverage of native forest, and especially the high precipitation values for the entire basin make the ZRB, as a whole, a vital recharge area for the Amazon foothills.

The ultimate goal of GIS-based groundwater recharge analysis is not to present a definitive recharge map of the ZRB but to show a simplified representation of reality to help predict the impacts of anthropogenic activity in the basin. It mainly considers land-use change processes and the dispersion of pollutants from mining that can affect the supply of surface and groundwater available to people living within the ZRB.

The most important groundwater recharge zones in the basin are located further east, next to the Condor Mountains. Some of Ecuador's large-scale mining projects are located in the Condor Mountains area. Although the effects or influences of mining on the groundwater regime are not yet well understood, the location of these mining projects above these potentially important groundwater recharge zones poses a serious contamination hazard. Activities such as the disposal of wastewater from plants, pumping water from the mine, or washing waste and tailings dumps are potential sources of heavy metal contamination for groundwater (Raghavendra & Deka, 2015).

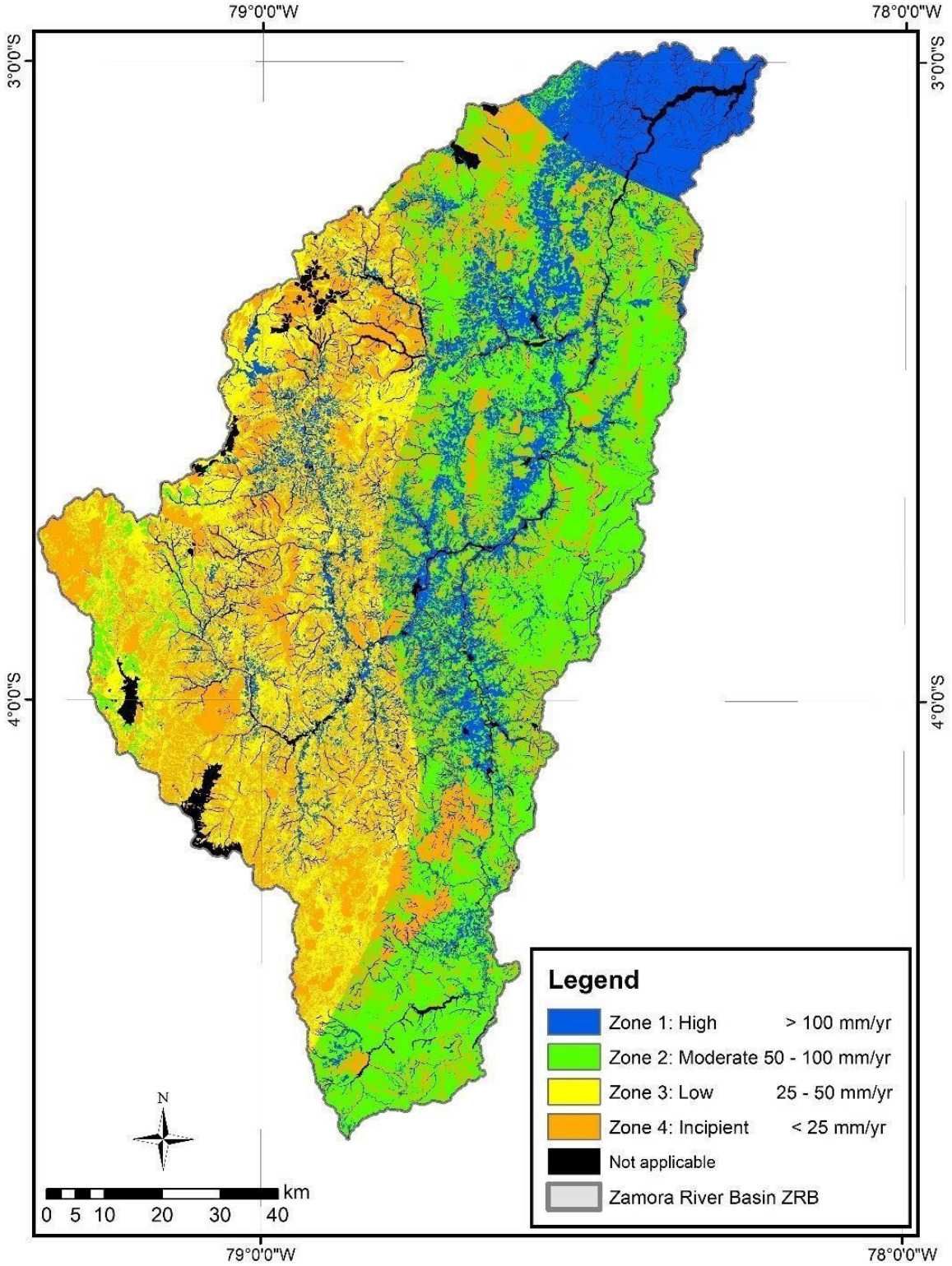


Fig. 10 Final groundwater recharge map of Zamora River Basin ZRB. Potential recharge ratios according to soil, land cover, and slope characteristics, and the precipitation of the area.

4.2. Recharge Conceptual Model using stable isotopes $\delta^{18}O$ and $\delta^{2}H$

The stable isotope data for precipitation samples from ZRB ranged from −2.89‰ to −6.53‰ for δ18O and from −9.41‰ to −40.14‰ for δ2H (Table 4). The deuterium excess was between 10.53‰ and 13.71‰ (Table 4). The Local Meteorological Water Line (LMWL) built with the precipitation samples was δ2H = 8.32δ18O + 13.50 (Fig. 11) which were plotted above the GMWL (δ2H = 8δ18O + 10) (Fig. 11). The equation that describes the LMWL is similar to those described by (Garcia et al., 1998) in Méndez, 30 km north of ZRB, whose equation is (δ2H = 8.51δ18O +13.53) and similar to that described by Jimenez (2020) at the Ikiam meteorological station, 225 km north of ZRB, whose equation is (δ2H = 8.4δ18O + 15.37). Comparison of the regression line of the ZRB with the LMWLs of Méndez and Ikiam station showed that these three LMWLs are not statistically different (R2 = 0.99; p-value < 0.05 for both cases). The similarity of the isotopic composition of the precipitation from the Napo province (Ikiam station location) to Mendez and ZRB may indicate that the precipitation in this entire area of the Ecuadorian Amazon has the same origin. For the ZRB's LMWL, we only used stable isotope data from the rainy season of the basin, the equation that describes the LMWL may vary slightly with the data from the dry season.

Fractionation is the change in the isotopic composition of precipitation, which is influenced by the origin of air masses, elevation, continentality, and latitude. The isotopic composition alteration is also by the climatic patterns of unique precipitation events (Crawford et al., 2013). Continentality is one factor that explains the substantial depletion of isotopes; the further an air mass moves inland; precipitation becomes more negative with a deficit of heavier isotopes, the further an air mass moves inland (Dansgaard, 1964). But for the ZRB, the altitudinal effect is the most influential factor that favors the depletion of isotopes in precipitation. As the humidity from the Amazon plain passes over an orographic barrier, such as the Andes Mountains, it is forced upwards, the temperature reduces, which favors preferential rainfall and the depletion of heavy isotopes (Dansgaard, 1964). The altitudinal effect of δ18O in the basin is evident; at a lower altitude, there is an enrichment of δ18O in the water samples and vice versa. Although for point P4, there is an exaggerated enrichment due to other factors such as water recycling processes. The average of the altitudinal isotopic gradient of the ZRB for every 100 m is -0.17, and this result is consistent with the altitude isotopes gradient of Garcia et al. (1998) and Maldonado-Astudillo et al. (1995).

Table 4 Isotopic composition in precipitation samples of ECU7007 project.

ID	Elevation	Date	$\delta^{18}O$ (‰)	$\delta^{2}H$ (‰)	d-excess (‰)
P1	2525	1/20/2018	-6.53	-40.14	12.10
P2	2160	11/28/2018	-6.41	-39.84	11.44
P3	1835	1/21/2018	-5.57	-33.14	11.42
P4	837	1/20/2018	-2.89	-9.41	13.71
P5	766	1/19/2018	-4.14	-22.59	10.53

The LMWL constructed from the precipitation samples (Fig. 11) shows that there are two types of precipitation samples: the Andean group (P1, P2, and P3 in Fig. 8A), which records the most impoverished δ18O values, and the Amazon group (P4 and P5 in Fig. 8A), which has the most enriched δ18O values. It becomes noticeable that the isotopic signature of the surface and spring water samples are closer to the Andean group (Fig. 11). This depletion of δ18O in the Andean group is mainly due to the altitudinal effect; the samples of this group register altitudes higher than 1800 m.a.s.l., and those of the Amazon group have elevations lower than 850 m.a.s.l.

Dansgaard (1964) established deuterium as an indicator of the source region of precipitation and the variations with the source area. The trajectories of air masses and areas of moisture sources can be traced with deuterium to improve our understanding of regional climate systems (Jansson et al., 2007). Deuterium has the property of changing seasonally; generally, warm-dry sources show high values, and cold-humid sources show low values. The average d-excess detected in our samples (11.86 ‰), and values that vary from 10.51 ‰ to 13.73 ‰ (Table 5) indicate that the source of moisture may come from the Amazon plain. According to Salati et al. (1979), the deuterium of the air masses that cross the Amazon remains in a range of 9.80 to 14.60 (‰), thus confirming the results.

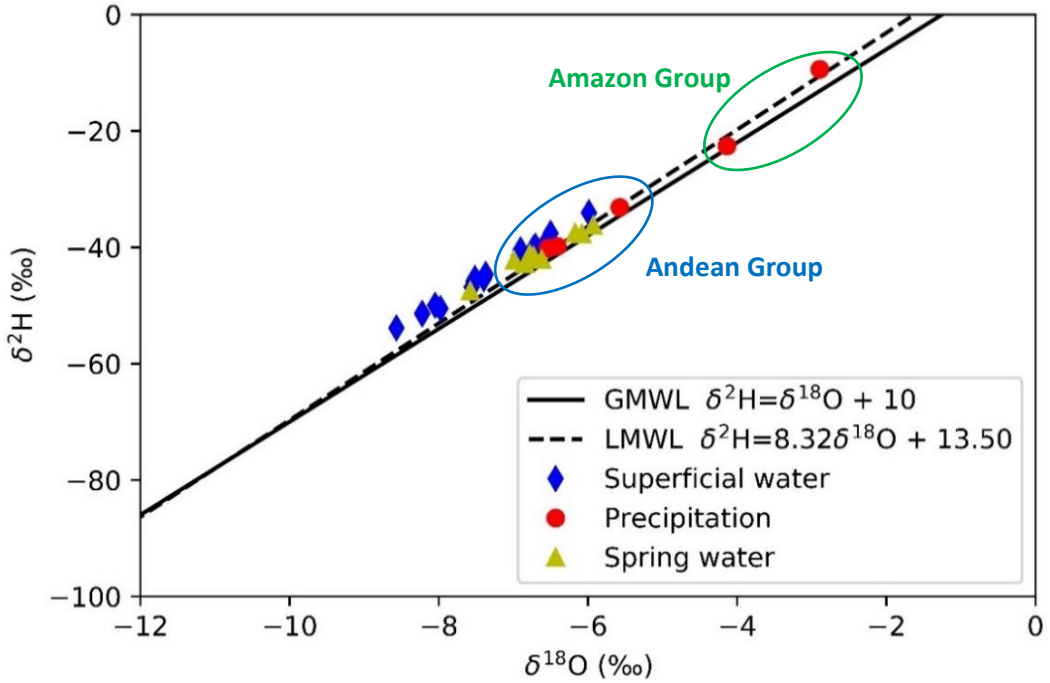


Fig. 11 LMWL and relationship between $\delta^{18}O$ and $\delta^{2}H$ in precipitation, superficial water, and spring water in Zamora River Basin (ZRB)

However, the sample point P4 (Fig. 8A) presents a value > 13‰, which is unusually higher than the remaining sample points of the Andean group, suggesting recycling processes within the basin. The d-excess for all surface water samples is also > 13 ‰ which is an indication that the surface water that runs through the watershed has undergone recycling processes. The documentation of recycling processes exists for the entire Amazon basin (Salati et al., 1979; Victoria et al., 1991). Since the ZRB is limited to the west by the Andes and the east by the Condor Mountains (Fig. 12), a recirculation process may be a persistent feature. Formost samples, the d-excess of spring water is between 8 and 12 ‰, typical of meteoric processes. However, there are three spring water points (G1, G3, and G6 in Fig. 8C) with a d-excess> 13 ‰. According to the sampling, the groundwater recharge processes in the ZRB are governed mainly bythe regional precipitation of the Amazon basin that comes from the Atlantic Ocean and crosses the entire Amazon until it collides with the Andes Mountains (Fig. 12) (Victoria et al., 1991).

The isotopic signature of the spring water samples is close to the precipitation samples of the Andean group (Table 5) (Fig. 11). We have already established that the source of the precipitation of the Andean group is the humidity coming from the Amazonian plain and probably from recycling processes within the ZRB (Fig.12) (Cabrera et al., 2021). Then we can establish that the primary source of groundwater recharge of the ZRB is the precipitation from the Amazon basin and the

precipitation from recycling processes within the basin. The stable isotopes indicate that for groundwater samples collected from, there are no surface water inputs (infiltrated from large water bodies, leaking water distribution systems, or irrigation activities) but rather the source of groundwater recharge for the ZRB is precipitation. If the source of groundwater recharge in the basin is precipitation, using the climatic water balance such as that of Thornthwaite & Mather (1955) is an excellent approximation to estimate recharge values.

Table 5 Statistical summary of isotopic table compositions in precipitation, superficial, and spring water samples in Zamora River Basin (ZRB).

Precipitation (n=5)	δ^2H (‰)	$\delta^{18}O$ (‰)	d-excess (‰)
Min	-40.14	-6.53	10.51
Max	-9.41	-2.89	13.73
Mean	-29.02	-5.11	11.86
Std	13.07	1.57	1.20
Superficial water (n=18)			
Min	-53.88	-8.57	13.21
Max	-34.06	-5.99	14.77
Mean	-44.35	-7.30	14.05
Std	5.58	0.72	0.50
Springwater (n=10)			
Min	-47.52	-7.58	10.87
Max	-36.25	-5.93	13.60
Mean	-41.08	-6.65	12.12
Std	3.25	0.49	0.95

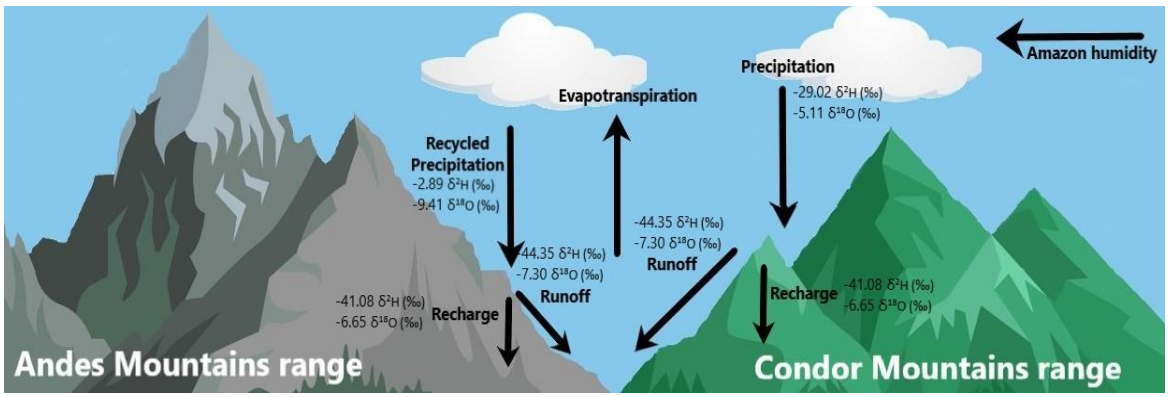


Fig. 12 Groundwater recharge conceptual model for ZRB and the mean of the isotopic composition of the study samples.

5. Conclusions

This study attempts to establish the relationship between the different factors influencing groundwater recharge and a GIS-based distributed water balance model to produce a groundwater recharge potential map and apply it to a large-scale basin, such as the ZRB. The applied method proves to be a helpful tool to estimate groundwater recharge, especially for areas with little or no hydrogeological information available.

The soil of the ZRB is mainly waterproof (high clay content); however, because of the low slopes <7% and native forest cover, the groundwater recharge is enhanced for the ZRB. Despite the importance of the soil type, precipitation is the single most significant driver of groundwater recharge in the ZRB. The high precipitation rates make the basin covered with high(18.22%) and moderate (30.93%) recharge zones.

The results indicated that the most effective groundwater recharge potential zone is downstream, located at the outlet of the basin in block six. In this block, the abundant precipitation allows high groundwater recharge rates that can reach more than 640 mm/yr. The fact that the mining activity is located in this vital groundwater recharge area poses a constant danger to the water quality of the Amazon basin. We must consider that some of the most important mining projectsin Ecuador operate in this area located in the northern part of the Condor Mountains. The pollutants from mining could be transferred in groundwater from the ZRB to the following basins, such as the Santiago River basin and Peruvian territory.

The stable isotopes data ($\delta^{18}O$ and $\delta^{2}H$) data indicate that most of the rainfall that precipitates in the basin comes from moisture transported from the Amazon plain and there are also recycling processes in the ZRB. They also indicate that the principal groundwater recharge comes from the precipitation from Amazon humidity and recirculation processes within the ZRB. This information is consistent with other stable isotope studies conducted in the Amazon region of Ecuador. However, we know that a broader sampling of the isotopic composition is required both temporally and spatially to confirm the model.

References

Allison, G. B. (1988). A Review of Some of the Physical, Chemical and Isotopic Techniques Available for Estimating Groundwater Recharge. *Estimation of Natural Groundwater Recharge*, 49–72. https://doi.org/10.1007/978-94-015-7780-9_4

Andreo, B., Vías, J., Durán, J. J., Jiménez, P., López-Geta, J. A., & Carrasco, F. (2008). Methodology for groundwater recharge assessment in carbonate aquifers: Application to pilot sites in southern Spain. *Hydrogeology Journal*, *16*(5), 911–925. https://doi.org/10.1007/s10040-008-0274-5

ASCE-American Society of Civil Engineers. (1969). Effect of urban development on flood discharges. Current knowledge and future needs. *Journal of the Hydraulics Division*, *95*(HY1), 287–309.

Avcı, D., & Fernández-Salvador, C. (2016). Territorial dynamics and local resistance: Two mining conflicts in Ecuador compared. *Extractive Industries and Society*, *3*(4), 912–921. https://doi.org/10.1016/j.exis.2016.10.007

Blasch, K. W., & Bryson, J. R. (2007). Distinguishing sources of ground water recharge by using δ2H and δ18O. *Groundwater*, *45*(3), 294–308. https://doi.org/10.1111/J.1745-6584.2006.00289.X

Brkić, Ž., Briški, M., & Marković, T. (2016). Use of hydrochemistry and isotopes for improving the knowledge of groundwater flow in a semiconfined aquifer system of the Eastern Slavonia (Croatia). *Catena*, *142*, 153–165. https://doi.org/10.1016/j.catena.2016.03.010

Cabrera, M., Moulatlet, G. M., Valencia, B. G., Maisincho, L., Rodríguez-Barroso, R., Albendín, G., Sakali, A., Lucas-Solis, O., Conicelli, B., & Capparelli, M. V. (2021). Microplastics in a tropical Andean Glacier: A transportation process across the Amazon basin? *Science of The Total Environment*, *805*, 150334. https://doi.org/10.1016/j.scitotenv.2021.150334

Chang, K. T., & Tsai, B. W. (1991). The effect of dem resolution on slope and aspect mapping. *Cartography and Geographic Information Systems*, *18*(1), 69–77. https://doi.org/10.1559/152304091783805626

Conicelli, B., Hirata, R., Galvão, P., Bernardino, M., Simonato, M., Abreu, M. C., Aranda, N., & Terada, R. (2021). Determining groundwater availability and aquifer recharge using GIS in a highly urbanized watershed. *Journal of South American Earth Sciences*, *106*. https://doi.org/10.1016/j.jsames.2020.103093

Copernicus Climate Change Service (C3S). (2017). *ERA5: Fifth generation of ECMWF atmospheric reanalyses of the global climate*. . . Copernicus Climate Change Service Climate Data Store

(CDS). https://cds.climate.copernicus.eu/cdsapp#!/home

Crawford, J., Hughes, C. E., & Parkes, S. D. (2013). Is the isotopic composition of event based precipitation driven by moisture source or synoptic scale weather in the Sydney Basin, Australia? *Journal of Hydrology*, *507*, 213–226. https://doi.org/10.1016/j.jhydrol.2013.10.031

Dansgaard, W. (1964). Stable isotopes in precipitation. *Tellus*, *16*(4), 436–468. https://doi.org/10.1111/J.2153-3490.1964.TB00181.X

de Oliveira Aparecido, L. E., de Souza Rolim, G., & da Silva Cabral de Moraes, J. R. (2020). Validation of ECMWF climatic data, 1979–2017, and implications for modelling water balance for tropical climates. *International Journal of Climatology*, *40*(15), 6646–6665. https://doi.org/10.1002/joc.6604

Dripps, W. R., & Bradbury, K. R. (2007). A simple daily soil-water balance model for estimating the spatial and temporal distribution of groundwater recharge in temperate humid areas. *Hydrogeology Journal*, *15*(3), 433–444. https://doi.org/10.1007/s10040-007-0160-6

El Khalil, H., El Hamiani, O., Bitton, G., Ouazzani, N., & Boularbah, A. (2008). Heavy metal contamination from mining sites in South Morocco: Monitoring metal content and toxicity of soil runoff and groundwater. *Environmental Monitoring and Assessment*, *136*(1–3), 147–160. https://doi.org/10.1007/s10661-007-9671-9

Erazo, B., Bourrel, L., Frappart, F., Chimborazo, O., Labat, D., Dominguez-Granda, L., Matamoros, D., & Mejia, R. (2018). Validation of satellite estimates (Tropical Rainfall Measuring Mission, TRMM) for rainfall variability over the Pacific slope and Coast of Ecuador. *Water (Switzerland)*, *10*(2). https://doi.org/10.3390/w10020213

Fenn, D., Hanley, K., & DeGeare, T. (1975). *Use of the water-balance method for predicting leachate generation from solid-waste-disposal sites*. https://www.osti.gov/biblio/6328350

Freeze, R. A., & Cherry, J. A. (1979). *Groundwater*. Prentice-Hall.

Galvão, P., Hirata, R., & Conicelli, B. (2018). Estimating groundwater recharge using GIS-based distributed water balance model in an environmental protection area in the city of Sete Lagoas (MG), Brazil. *Environmental Earth Sciences*, *77*(10), 1–19. https://doi.org/10.1007/s12665-018-7579-z

Garcia, M., Villalba, F., Araguas Araguas, L., & Rozanski, K. (1998). The role of atmospheric circulation patterns in controlling the regional distribution of stable isotope contents in precipitation: Preliminary results from two transects in the Ecuadorian Andes. *Isotope Techniques in the Study of Environmental Change. Proceedings of a Symposium, Vienna, April*

1997., 127–140. https://inis.iaea.org/Search/search.aspx?orig_q=RN:29044418

Healy, R. W., & Scanlon, B. R. (2011). Estimating groundwater recharge. In *Estimating Groundwater Recharge* (Vol. 9780521863). https://doi.org/10.1017/CBO9780511780745

Heilweil, V. M., Solomon, K. D., Gingerich, S. B., & Verstraeten, I. M. (2009). Oxygen, hydrogen, and helium isotopes for investigating groundwater systems of the Cape Verde Islands, West Africa. *Hydrogeology Journal*, *17*(5), 1157–1174. https://doi.org/10.1007/S10040-009-0434-2

Hendrickx, J. M. H. (1992). Groundwater Recharge. A Guide to Understanding and Estimating Natural Recharge (Volume 8, International Contributions to Hydrogeology). *Journal of Environmental Quality*, *21*(3), 512–512. https://doi.org/10.2134/jeq1992.00472425002100030036x

Jansson, P., Linderholm, H. W., Pettersson, R., Karlin, T., & Mörth, C. M. (2007). Assessing the possibility to couple the chemical signal in winter snow on Storglaciären, Sweden, to atmospheric climatology. *Annals of Glaciology*, *46*, 335–341. https://doi.org/10.3189/172756407782871459

Jasrotia, A. S., Kumar, R., & Saraf, A. K. (2007). Delineation of groundwater recharge sites using integrated remote sensing and GIS in Jammu district, India. *International Journal of Remote Sensing*, *28*(22), 5019–5036. https://doi.org/10.1080/01431160701264276

Koerner, R., & Daniel, D. (1997). Final Covers for Solid Waste Landfills and Abandoned Dumps. In *Final Covers for Solid Waste Landfills and Abandoned Dumps*. https://doi.org/10.1680/fcfswlaad.9780784402610

Liu, F., Song, X., Zhen, P., Wang, L., & Wang, S. (2019). Insights from stable isotopes of water and hydrochemistry to the evolutionary processes of groundwater in the Subei lake basin, Ordos energy base, Northwestern China. *Isotopes in Environmental and Health Studies*, *55*(5), 438–458. https://doi.org/10.1080/10256016.2019.1654472

Maldonado-Astudillo, S., Cepeda-Tobar, H., & Araguas-Araguas, L. (1995). Hydrogeological and isotopic study of the Guayas river Delta aquifers (Ecuador); Estudio hidrogeologico e isotopico de los acuiferos del Delta del Rio Guayas. (in Spanish). *International Atomic Energy Agency*, *27*(6), 195–209. https://inis.iaea.org/search/search.aspx?orig_q=RN:27018956

Mazor, E. (2004). Chemical and Isotopic Groundwater Hydrology Third Edition. In *Applied Chemical and Isotopic Groundwater Hydrology*. https://books.google.es/books?hl=es&lr=&id=AUND-o9klhMC&oi=fnd&pg=PR3&dq=Chemical+and+isotopic+groundwater+recharge&ots=d0j7wa

8kv8&sig=3F7N1r0LLiZ43ssnhmnyL9YPnnY

Melo, C., Mena, C. F., Arsel, M., & Pellegrini, L. (2013). The State is dead, Long Live the State: Re-inserting the State in the Gold-mining Industry in Zamora-Chinchipe, Ecuador. *CoCooN NEBE Working Paper*, 1–37. https://doi.org/10.13140/RG.2.1.3891.7603

Mora, A., Jumbo-Flores, D., González-Merizalde, M., Bermeo-Flores, S. A., Alvarez-Figueroa, P., Mahlknecht, J., & Hernández-Antonio, A. (2019). Heavy Metal Enrichment Factors in Fluvial Sediments of an Amazonian Basin Impacted by Gold Mining. *Bulletin of Environmental Contamination and Toxicology*, *102*(2), 210–217. https://doi.org/10.1007/s00128-019-02545-w

Mora, A., Jumbo Flores, D., & Mahlknecht, J. (2018). Levels of MN, ZN, PB and HG in sediments of the zamora river, Ecuador. *Revista Internacional de Contaminacion Ambiental*, *34*, 245–249. https://www.researchgate.net/profile/Diogenes-Hernandez-3/publication/330141509_Characterizing_the_evolution_of_sediment_like_wastes_exposed_to_ambient_conditions_in_open_reservoirs/links/5c2f5b6da6fdccd6b590bf0c/Characterizing-the-evolution-of-sediment-l

Nolan, B. T., Healy, R. W., Taber, P. E., Perkins, K., Hitt, K. J., & Wolock, D. M. (2007). Factors influencing ground-water recharge in the eastern United States. *Journal of Hydrology*, *332*(1–2), 187–205. https://doi.org/10.1016/j.jhydrol.2006.06.029

Pereira, A. R. (2005). Simplificando o balanco hidrico de Thornthwaite and Mather. *Bragantia*, *64*(2), 311–313.

Raghavendra, N. S., & Deka, P. C. (2015). Sustainable Development and Management of Groundwater Resources in Mining Affected Areas: A Review. *Procedia Earth and Planetary Science*, *11*, 598–604. https://doi.org/10.1016/j.proeps.2015.06.061

Rwanga, S., (IJAAEE), J. N.-I. J. A. A. E. E., & 2017, U. (2017). Approach to Quantify Groundwater Recharge Using GIS Based Water Balance Model: A Review. *International Journal of Research in Chemical, Metallurgical and Civil Engineering*, *4*(1). https://doi.org/10.15242/ijrcmce.ae0317115

Salati, E., Dall'Olio, A., Matsui, E., & Gat, J. R. (1979). Recycling of water in the Amazon Basin: An isotopic study. *Water Resources Research*, *15*(5), 1250–1258. https://doi.org/10.1029/WR015i005p01250

Scanlon, B. R., Healy, R. W., & Cook, P. G. (2002). Choosing appropriate techniques for quantifying groundwater recharge. *Hydrogeology Journal*, *10*(1), 18–39. https://doi.org/10.1007/s10040-001-0176-2

Thornthwaite, C. W., & Mather, J. R. (1955). The water balance. Laboratory of Climatology Report No. 8. *Drexel Institute of Technology, New Jersey, USA*.

Torracchi, J. (2015). *Deforestación y Pérdida de hábitat en Bosques de montaña en la Cuenca alta del Río Zamora (Loja, Ecuador)*. https://dialnet.unirioja.es/servlet/tesis?codigo=116354

Tropical Rainfall Measuring Mission (TRMM). (2011). *TRMM (TMPA) Rainfall Estimate L3 3 hour 0.25 degree x 0.25 degree V7*. Goddard Earth Sciences Data and Information Services Center (GES DISC). https://doi.org/10.5067/TRMM/TMPA/3H/7

van Teijlingen, K., & Hogenboom, B. (2016). Debating Alternative Development at the Mining Frontier: Buen Vivir and the Conflict around El Mirador Mine in Ecuador. *Journal of Developing Societies*, *32*(4), 382–420. https://doi.org/10.1177/0169796X16667190

Victoria, R. L., Martinelli, L. A., Mortatti, J., & Richey, J. (1991). Mechanisms of water recycling in the Amazon basin: isotopic insights. *Ambio*, *20*(8), 384–387. https://doi.org/10.2307/4313869

Villa-Achupallas, M., Rosado, D., Aguilar, S., & Galindo-Riaño, M. D. (2018). Water quality in the tropical Andes hotspot: The Yacuambi river (southeastern Ecuador). *Science of the Total Environment*, *633*, 50–58. https://doi.org/10.1016/j.scitotenv.2018.03.165

Wood, W. W. (1999). Use and misuse of the chloride-mass balance method in estimating ground water recharge. In *Ground Water* (Vol. 37, Issue 1, pp. 2–3). National Ground Water Association. https://doi.org/10.1111/j.1745-6584.1999.tb00949.x

Yeh, H. F., Lin, H. I., Lee, C. H., Hsu, K. C., & Wu, C. S. (2014). Identifying seasonal groundwater recharge using environmental stable isotopes. *Water (Switzerland)*, *6*(10), 2849–2861. https://doi.org/10.3390/w6102849

Yeh, H. F., Lin, H. I., Lee, S. T., Chang, M. H., Hsu, K. C., & Lee, C. H. (2014). GIS and SBF for estimating groundwater recharge of a mountainous basin in the Wu River watershed, Taiwan. *Journal of Earth System Science*, *123*(3), 503–516. https://doi.org/10.1007/s12040-014-0420-5

Yin, L., Hou, G., Su, X. S., Wang, D., Dong, J., Hao, Y., & Wang, X. (2011). Isotopes (δD and δ18O) in precipitation, groundwater and surface water in the Ordos Plateau, China: Implications with respect to groundwater recharge and circulation. *Hydrogeology Journal*, *19*(2), 429–443. https://doi.org/10.1007/S10040-010-0671-4